IEEE Access
Multidisciplinary | Rapid Review | Open Access Journal

IEEE VEHICULAR TECHNOLOGY SOCIETY SECTION

Received 5 October 2022, accepted 14 October 2022, date of publication 26 October 2022, date of current version 3 November 2022.

Digital Object Identifier 10.1109/ACCESS.2022.3217214

RESEARCH ARTICLE

New Decentralized Actuator System Design and Control for Cost-Effective Active Suspension

JEONG-WOO LEE[1] AND KWANGSEOK OH[2], (Member, IEEE)

[1]Research and Development Center, Bundang-gu, Seongnam-si, Gyeonggi-do 13486, Republic of Korea
[2]School of ICT, Robotics & Mechanical Engineering, Hankyong National University, Anseong-si, Gyeonggi-do 17579, Republic of Korea

Corresponding author: Kwangseok Oh (oks@hknu.ac.kr)

ABSTRACT A new active suspension control system that replaces the existing complex hydraulic systems was proposed in this paper by reviewing recent research and development trends. We studied the actuator system characteristics, force, and damping control by conducting studies on actuator dynamics, which are yet to be studied in the literature. Moreover, many damping and active force mechanism concept studies have been conducted based on several proposed hydraulic circuits. Based on the conducted studies, a new decentralized actuator system was designed for compact and efficient vehicle control. For the piecewise control, a model-based actuator force control algorithm was proposed with consideration of the individual main component non-linearity for force application scalability. Based on a semi-active system applied to the existing commercialization, the on-demand electric pump at each wheel is integrated into the system circuit to propose a realistic, cost-effective solution. Additionally, from the vehicle control point of view, an integrated control algorithm for active suspension was developed using a model-based control method and conventional map-based inverse control methods, considering nonlinear actuator characteristics and road input disturbance. Finally, the performance of the proposed control system was evaluated using a simulation technique and an actual test platform.

INDEX TERMS Active suspension, actuator dynamic control, decentralized actuator system, feedback and feed-forward control, nonlinear model-based force control.

I. INTRODUCTION

Much research has been conducted on active suspension systems to improve vehicle ride comfort and maneuver stability simultaneously. Since the 1990s, several OEMs(Original Equipment Manufacturers) have proposed successful commercialization systems of active suspension. However, they are yet to be popularized owing to the complexity of the system, price constraints, and limitations in system performance improvement [1]. However, since 2013, the development of the active suspension system has received renewed attention. This can be attributed to the trend of vehicle electrification and the expectation of new improvements in vehicle performance owing to the development of autonomous driving functions. The main research direction of active suspension can be divided into two parts: 1) package improvement and 2) actuator system simplification architecture for generating required force and improving riding comfort and vehicle attitude control effects through force control performance improvement. The primary research can be summarized as power electrification, and the system configuration can be integrated with the existing suspension elements.

A. PREVIOUS ACTUATION SYSTEM APPLICATION

The first commercial application was to control the hydraulic actuator force through a hydraulic pump driven by an engine, a hydraulic pressure control valve, and a flow control valve. The actuator force control is a structure that uses a single-acting hydraulic actuator. The spring effect occurs when a damping force is generated due to the accumulator stiffness. In addition, various hydraulic condition monitoring systems are required to ensure hydraulic control [2]. In the 2000s, a system was proposed in which hydraulic actuators were installed within the general coil-spring damper assembly

The associate editor coordinating the review of this manuscript and approving it for publication was Ton Duc Do.

structure to generate active force through spring displacement control. Therefore, the response of the actuator system was directly related to the stiffness of the connected suspension. Although an improvement in force control performance has been proposed, the basic hydraulic system configuration is similar to that of traditional hydraulic circuits and sensors [3].

Since 2013, research has been conducted to develop a system that can reduce the complexity of the traditional hydraulic system and improve its performance. First, a study was conducted to improve the system performance by integrating a semi-active damper with an existing commercial active-force actuator element. This system is an example of performance improvement through independent active and damping force control [4]. Second, TNO, one of the institutes researching advanced suspension systems, proposed an independent system for active force control through independent hydraulic control of each damper tension/compression chamber using a centralized pump [5].

The damper structure was configured as an active suspension system to remove the conventional hydraulic circuit in the damper manufacturing company. Research is being conducted to drive the pump using a motor synchronized with damper operation to create an active force. The research subject focused on system performance improvement by changing the damper actuator hydraulic circuit. Furthermore, it concentrated on developing a method integrated with the damper by improving the pump function. In addition, a study was also conducted to increase the overall system efficiency using regenerative damping of the energy consumed during active force control [6].

B. PREVIOUS SYSTEM CONTROL

In previous studies, considerable research has been conducted on developing control algorithms to improve performance from a vehicle perspective. In the existing control system application studies, active suspension research cases can be divided into four parts such as optimal, adaptive, nonlinear, and H-infinity controls. Optimal control generally defines vehicle ride comfort and driving stability as a cost function and calculates the control gain based on the linear quadratic regulator. Adaptive control estimates the actuator–damper speed or dynamic wheel load in active and semi-active suspension systems. Therefore, the estimator affects the control performance via gain scheduling. If the effect of the internal actuator dynamics is significant, the vehicle control performance may deteriorate owing to modeling error and improper determination of the adaptation rate. Finally, actuation system force control was studied from the perspective of hydraulic pressure control in the traditional hydraulic system configuration. Sliding-mode control is realistically applied with uncertainty, and in the case of active suspension, it is primarily used for active force tracking control. [7] It is well known that chattering and undeserved energy inputs can be issued when controlling the sliding mode owing to model and parameter adaptation and disturbance boundary uncertainty.

C. RESEARCH OUTLINE

This study proposed a new decentralized active suspension actuator structure, including an active-force-generating structure, and its performance was verified through simulation and actual platform-based testing. Furthermore, a new actuator system architecture for damping and active mode functionality was also proposed based on key functional requirements analysis and performance validation.

We propose a controller that considers the nonlinear characteristics of each component to implement a precise force control based on the proposed system structure. The nonlinear adaptive actuator model-based control was implemented by considering the empirical map and dynamic model for the components composed of the actuator assembly, such as valves and motor pumps. The proposed control scheme ensures scalability for various types of vehicles, and a reasonable control performance can be sustained despite the performance degradation of the vehicle using the designed nonlinear characteristics with the adaptation method. An important parameter, such as damper speed, is estimated to implement the force-tracking control algorithm. From a power control point of view, it can be defined as electric-hydraulic control based on motor control. As a result, the control accuracy and efficiency are improved compared to the existing nonlinear valve-control-based pressure control. Based on the designed nonlinear model-based adaptive actuator controller, an active suspension actuator system that simplifies the existing hydraulic system configuration and is advantageous for power efficiency and independent control was proposed.

The main contributions of this study are summarized as follows.

1) A new decentralized actuator system was designed for compact and efficient control.
2) Model-based actuator force control algorithm was proposed for the piecewise control considering the individual main component non-linearity for force application scalability.

The remainder of this paper is organized as follows. Section 2 presents a brief review of the active suspension system architecture, and Section 3 describes the design method of the actuator system. In Section 4, the modeling- and simulation-based evaluation results of the actuator system are described. Section 5 explains the integrated control algorithm of the active suspension actuator, and Section 6 describes the simulation and actual test platform-based validation results of the actuator force control. Finally, the concluding remarks are given along with the future scope in Section 7.

II. BRIEF REVIEW OF ACTIVE SUSPENSION SYSTEM ARCHITECTURE

A. FUNCTION REQUIREMENTS

The suspension system of a vehicle must provide three major functions:

1. It must effectively block the irregular disturbances of the surface of the road while driving the vehicle, and it must be able to deliver a comfortable ride to the driver in the appropriate frequency range.
2. The driver's comfort should be taken care of by effectively controlling the change in vehicle attitude caused by the driver's input or the road environment.
3. Steering stability should be ensured by maintaining the road-holding ability of the tire when driving on uneven roads.

A plethora of research has been conducted to maximize the performance of the above-described metrics since the 1990s. As a part of this, the chassis system was improved by changing the damper and spring characteristics. The damper is a key actuator that constitutes the semi-active suspension system, and the damping force is varied through solenoid valve control with low power consumption. Much research has been carried out to this end, along with the application of Skyhook control theory, and it occupies most of the commercialized electronically controlled suspensions [8], [9], [10]. An *active suspension* is a system that actively changes the wheel movement and vehicle motion using additional power. Even though the need for an additional power source for the control operation, several realistic constraints exist, such as system configuration complexity, weight, and overall system efficiency. Practical and academic research on this topic was conducted for the first time in 1990. However, there was some deterioration in ride quality with the imitation of hydraulic and electronic control technology, and hence, it did not get popular in the market [11], [12].

B. PERFORMANCE REVIEW OF THE VARIOUS ACTIVE SUSPENSIONS

Some problems of the active suspension systems include a discontinuity in attitude control due to active control disharmony with the damping function and, second, deterioration of ride comfort due to high internal pressure and friction of parts. In addition, pump operation using the vehicle's engine power has a disadvantage in terms of the overall vehicle fuel economy. As of the late 2000s and early 2010s, researchers focused on developing new actuation systems to improve the current active suspension dynamics and complexity [13], [14], [15], [16], [17], [18], [19], [20]. The main focus was the architecture and control of the actuator system. Developing an actuator control system that integrates active force and damping function control is mainstream regarding vehicle dynamics. In this chapter, the characteristics of the active suspension system and advanced actuator control system, currently under study by industrial or academic research, are investigated. Through this survey, the functional and component requirements of the active suspension actuator system were summarized according to the increasing trend of autonomous driving and electric vehicles. The system efficiency is directly related to the efficiency of the power conversion components, and the reliability is based on the endurance of the existing application of automotive vehicles. The electromagnetic-force-creating mechanism that directly uses a motor has the best system efficiency, but it is disadvantageous in terms of damping characteristics, cost, and mass. The damping implementation considered that the hydraulic type is appropriate given the current performance requirements. Considering the cost, system reliability, and damping capability, the valve-damping-based electro-hydrostatic active suspension system is judged to be the most reasonable concept. Based on the above description, each system topology can be qualitatively evaluated and summarized in terms of the Pugh matrix evaluation from the upper, lower, and middle viewpoints. Table 1 shows a comparison of the active suspensions.

TABLE 1. Comparison table between active suspensions.

Feature	Hydraulic damping			Motor-driven damping		
Architecture & Configuration	Series type	Parallel type	Electro-hydrostatic	Electro-mechanical (rotary type)	Electro-mechanical (ball screw type)	Electro-magnetic
Mass	+	++	++	+++	++	+
Complexity	+	+~++	++	++	+	+
Cost	+	+	+	++	+	+
Efficiency	++	++	++	++	++	+++
Damping flexibility	+++	+++	+	+	+	++
Control	++	++	++	++	++	+++
Reliability	+++	+++	++	+	+	+
Oil-free	No	No	No	Yes	Yes	Yes
Force density	+++	+++	+++	+	++	++
Bandwidth	+	+++	+++	+++	+++	+++

Based on the comparison results in Table 1, we propose a schematic of the new active suspension actuation system, as shown in Figure 1. Unlike the existing method of controlling one main hydraulic power using a pump and valve, the precision and simplification of control were performed by directly controlling the actuator force using a motor. There is a limit to the maximum number of times pressure can be controlled in the conventional case of a high-pressure accumulator; therefore, there is an additional operating mode to maintain high pressure. The proposed system integrates a simple pump structure with a damper to simplify the hydraulic complexity. This can be seen as more efficient because it generates only the necessary force at any time through on-demand motor control. In addition, because the existing conventional system creates a separate active pressure and fuses with the independent conventional damping function, the active force covers the entire control area. The proposed system combined an active-force generation model with a semi-active damping function. Performance efficiency can be improved by minimizing the active force generation

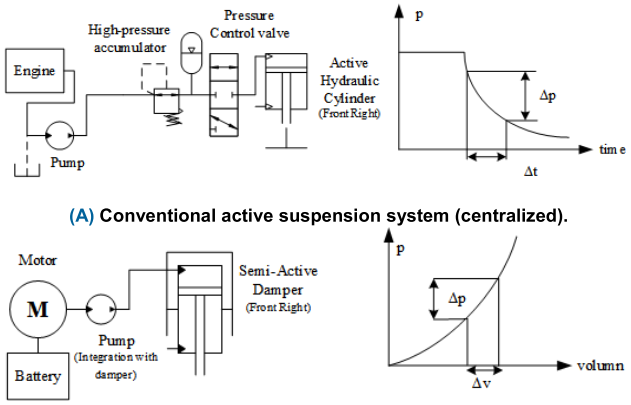

(A) Conventional active suspension system (centralized).

(B) Proposed suspension system (decentralized).

FIGURE 1. Active suspension system schematic comparison.

TABLE 2. Proposed system review.

System	Performance
Conventional active system	1. Centralized pump with hydraulic circuit 2. The control valve with a throttle determines the pressure gradient 3. The pressure changes Δp via time control 4. nonlinear dependent on the valve, pressure level
Proposed	1. decentralized pump integration with damper 2. The electric motor with semi-active damper dynamics determines Δp and pressure response. 3. Performance scalability via motor control software (torque and velocity control)

area. Fig. 1 shows the schematic comparison of the active suspension system.

III. SYSTEM DESIGN OF THE ACTUATOR SYSTEM

A. HYDRAULIC VALVE DAMPING

Mechanical damping using a valve transforms the kinetic energy generated by the road surface into thermal energy. This study applied a continuous damping control (CDC) valve that can control variable flow. Using the CDC valve, the wheel behavior damping function can be applied to high-frequency road inputs.

In addition, the CDC valves must be connected to the active module bidirectional pump by a hydraulic circuit, and they should have an independent hydraulic chamber. The maximum pressure of the pump and its pressure drop capability can be adjusted based on the CDC valve pressure-flow characteristics. This relationship is one of the design constraints in that the maximum pressure of the CDC valve in the firm mode should be higher than the maximum pump pressure. Fig. 2 shows the active actuator system designed in this study.

The actuator force requirements are defined by the maximum force and speed specifications. The force required to generate the maximum roll moment that compensates for the vehicle roll behavior is matched with the maximum actuator force value, and the speed can be defined as the point for

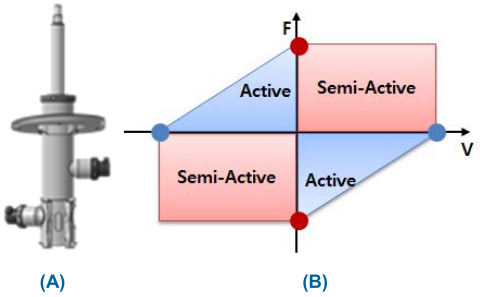

FIGURE 2. Designed active actuator system: (a) actuator assembly; (b) force characteristics schematic.

TABLE 3. Force requirements for the active suspension systems.

Requirement	Explanations
Active Force	1. Vehicle roll motion compensation under steering maneuver 2. Active ride control over the road 3. Piecewise force control for the accurate vehicle motion control
Damping	1. Soft damping 2. Large flow rate valve for soft damping Firm damping 3. Enough pressure build-up at a low flow rate to maintain active pump maximum pressure

possible active ride comfort control. Here, the quantitative value of the pressure flow rate may vary depending on the dimensions of the damper, but the considerations can be summarized as follows(Table 3):

B. ACTIVE FORCE MODULE

The pump is the proposed component that supplies flow to the damper actuator to generate an active force. The pressure determined by the motor pump power can be used to control the vehicle's behavior. Previous system configurations drove the pump using engine power, and one or two separate centralized pump modules were used. Because the system's active mode operation is performed by supplying power to the four-wheel actuator through hydraulic piping, the engine should be operated at all times, which affects the vehicle's fuel efficiency. Consequently, additional hydraulic circuitry components, such as pipe dynamics, affect the dynamic performance of the entire system. In this paper, we propose a power-on-demand type that uses a battery as a power source rather than an engine. We also propose a decentralized pump drive that eliminates the complexity of the intermediate system by integrating the motor pump into a four-wheel actuator. By independently operating the four-wheel pump, the dynamic response loss due to the previous hydraulic circuit piping characteristics can be reduced, and the degree of freedom of the control is also improved because it directly drives the required power for each actuator. In addition, it is a more advantageous configuration for optimization in terms of system power usage. Fig. 3 shows the components of the four-wheel independent active damper actuator.

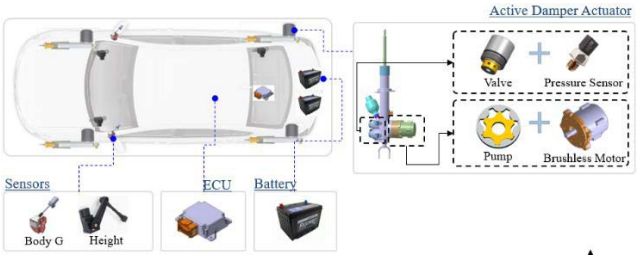

FIGURE 3. Four-wheel independent active damper actuator components.

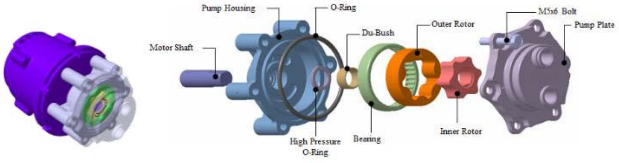

FIGURE 4. Gerotor pump for the active force module: (a) assembly; (b) exploded view.

The system requirements of the active force-generating module can be summarized as follows.

- More electrification
- High efficiency compared to conventional hydraulics
- Reduction in potential hydraulic loss due to leakage owing to the complex hydraulic circuit
- Piecewise control of actuator motion control (force, velocity, displacement)
- power-on-demand control
- option: potential energy regeneration

1) PUMP DYNAMICS

The motor pump design can be a deciding factor for the pressure, flow rate, and flow capacity that can be delivered. The buildup pressure of the pump should create a full range of active force of the actuator. The maximum active force should compensate for the vehicle's natural motion owing to ride and handling. In addition, the volume of the motor pump should be minimized as it is to be installed in each damper actuator layout. To this end, an internal motor pump, which is a volumetric pump consisting of only two elements, the inner and outer rotor, is proposed in this study. The total number of inner rotor teeth was less than that of the outer rotor, and the inner rotor centerline was located at a fixed eccentric position from the outer rotor centerline. Fig. 4 shows the gerotor-based internal pump split view of the component assembly, and table 4 shows the gerotor benefit of the active force module.

These fixed displacement devices offer important advantages as compared to other hydraulic pump types, such as reduced tooth wear, less number of components, and versatility for integration into any fluid power system. Moreover, they are suitable for the low-mid pressure range (up to 150 bar). Disadvantages include leakage issues according to the component speed and load pressure, sensitivity to major design parameters, and attention to durability at high rotations.

TABLE 4. Gerotor benefit of the active force module.

Advantages	Description
Cost-Effective	- Simplicity: The structure of housing and pocket is simple, so it is inexpensive and can be reduced to one shaft compared to spur gear type. It consists of two bearings and two seal - Small Package: Outer diameter and inner diameter length can be made small and optimized
Flexibility	It can be installed directly on the exit shaft, and the mating gear can drive the outer diameter
Performance	- Long service life: The relative speed between the inner and outer rotors is very low. As a result, wear can be minimized, and long life can be obtained. - Volumetric efficiency and high-speed - capability Balance: Each element rotates around its own centerline, so there is no inherent mechanical imbalance or interaction

2) DAMPER ACTUATOR

The performance and efficiency of an actuator vary depending on the damper module, damping force generation structure, and active power-module configuration. The hydraulic system consists of an accumulator, a reservoir, a variable valve, a motor pump, and additional hydraulic elements. The design considerations can be summarized as follows:

- Hydraulic circuit: the connection between the motor pump and damper actuator;
- Operation: pump operation direction;
- Pressure control: variable damping valve;
- Package;

The motor pump generates pressure by supplying additional flow to the damper actuator, flow chamber, compression chamber, and rebound chamber. In this case, the damper oil flow is an essential determinant of actual internal pressure generation. When the pump is connected to a damper, regenerative damping can be added, which directly affects the pressure and flow generation of the other valves. In the case of oil flow separation from regeneration, the flow rate is only discharged in the pump; thus, the influence on the system's operation is reduced, but an additional hydraulic circuit is required for the separation structure, increasing the complexity. The pump drive direction is related to the pressure generation and additional valve structure. When the flow rate is supplied in one direction, the force generated by the pressure area difference between the tension and compression is generated such that the generated force is less than that in bidirectional driving. However, in this case, it may be possible to change the direction through additional hydraulic valves, but this will affect the responsiveness of the hydraulic system and increase the complexity of the system. When the motor pump can be used for bidirectional control, the force can be generated as much as the hydraulic pressure area of

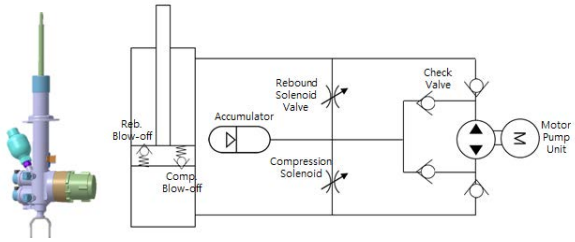

FIGURE 5. Proposed active suspension actuator circuit: (a) real proto assembly; (b) schematic of the system hydraulic circuit configuration.

each chamber; therefore, it is efficient in terms of active force generation. When the motor pump has bidirectional control, the force is created according to the equivalent area of each chamber, which is efficient in terms of active force generation. However, compensation should be made for the effect of the hydraulic oil dynamic property and mechanical inertia owing to bidirectional pump operation.

The CDC valve is a part of implementing the damping force, and its design consideration is the number of valves for the application and whether it is an internal or external application. The valve should have an operating mode to maintain the pressure when the active pump module is pressurized, and it should control the chamber pressure when switching to the damping force control mode. In the case of generating pressure and flow characteristics in the damping force mode, it is more advantageous to have a high tuning degree of freedom for the damping force and range of soft and firm damping forces. Also, to realize an active suspension force functionality, a large pressure difference between the maximum and minimum pressures of the valve should be provided.

IV. PHYSICAL MODELING AND SIMULATION OF THE ACTUATOR SYSTEM

Fig. 5 shows the actual proto assembly and the schematic of the hydraulic system circuit configuration proposed in this study.

DAMPING MODE (REBOUND STROKE)

The damper piston rod moves upward by road excitation in the rebound stroke mode. As a result, the generated flow is transferred to the rebound solenoid valve, and a damping force is generated when a pressure drop occurs through the valve. In addition, the flow rate of the rod volume generated by the piston rod in the rebound stroke was compensated for by the accumulator, and the flow rate was generated through the compression solenoid valve to supply the flow rate to the compression chamber. Because the flow path was blocked through the check valve on the motor pump side, the flow rate did not occur on the motor pump side. Therefore, the red line represents the high-pressure oil flow, and the blue line represents the low-pressure oil flow. Fig. 6 shows the circuit condition in case of the system operation mode is rebound damping.

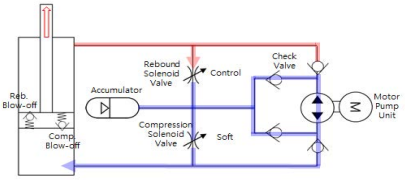

FIGURE 6. System operation mode: rebound damping.

The flow continuity equation of the rebound chamber in the rebound stroke is as follows:

$$A_c\dot{x}_{rod} - q_{cdc}^{reb} + \frac{V_r}{\beta}\dot{p}_r = 0$$
$$q_{cdc}^{reb} = C_d A_{cdc}\sqrt{\frac{2(p_{cdc}^{reb} - p_a)}{\rho}} \quad (1)$$

where A_c and V_r represent the cross-sectional area of the piston rod and volumetric displacement, respectively. And $\dot{x}_{rod}$ is the velocity of the piston rod. q_{cdc}^{reb} and $\dot{p}_r$ are the flow and pressure rates from the rebound chamber of the cylinder, respectively. β is the bulk modulus of the fluid. In (1), the flow rate can be calculated using the flow equation. where C_d, A_{cdc} are the flow coefficient and rebound solenoid valve orifice effective area, respectively. p_{cdc}^{reb}, p_a are the high pressures of the solenoid valve and the accumulator, respectively. ρ denotes the fluid density.

ACTIVE FORCE MODE (COMPRESSION STROKE)

In the active compression mode, a compression stroke is actively generated by pressurizing the tension chamber using the motor pump power. It is a principle to raise the pressure by supplying the flow rate to the tension-side chamber by taking the flow from the accumulator. Because the damping force variable valve is connected in parallel to the intermediate circuit, valve control should be carried out to minimize the valve oil leakage and pressure loss due to the flow loss. Generally, the flow rate is supplied using a motor pump by setting the valve pressure on the firm mode in which the valve orifice is the smallest. However, it is essential to rapidly discharge the pressure of the compression chamber to the accumulator side for fast active force build-up to increase the pressure difference. The solenoid variable valve on the compression side should be in the soft mode to ensure maximum flow. In addition, a blow-off valve is applied inside the damper to prevent the internal pressure of the actuator from excessively increasing under external shock and excessive working pressure conditions, thereby causing problems in the durability and performance of each subpart. Fig. 7 shows the circuit condition in case of the system operation mode is active force creation.

$$A_r\dot{x}_{rod} - q_{ces}^{reb} + q_{pump} - q_{leak}^{pump} + \frac{V_r}{\beta}\dot{p}_r = 0$$
$$q_{cdc}^{reb} = C_d A_{cdc}\sqrt{\frac{2(p_{cdc}^{reb} - p_a)}{\rho}} \quad (2)$$

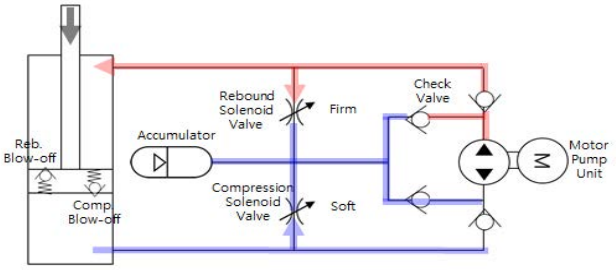

FIGURE 7. System operation mode: active force creation (compression stroke).

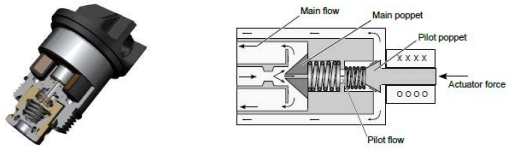

FIGURE 8. Continuous damping valve: (a) assembly; (b) schematic of the inner configuration; [20].

where q_{pump} and q_{leak}^{pump} are the pump and leakage flow rates, respectively. The pump is a positive-displacement gerotor pump, and the flow rate is defined as follows:

$$q_{pump} = D \times \omega_{pump}$$
$$D = \frac{dV}{d\theta} = H \cdot \frac{dA_{pump}}{d\theta} \tag{3}$$

where D is the change in flow volume, A_{pump} is the cross-sectional area of the flow rate, θ is the rotational angle of the pump rotor, ω_{pump} is pump rotational speed, and H is the thickness of the pump.

A. CONTINUOUS DAMPING CONTROL

The CES(Continuously controlled Electronic Suspension) valve is a pilot-operated pressure-control valve comprising two hydraulic stages. One is the main stage, and the other is the pilot stage. Through solenoid current control, the internal flow path orifice was controlled by the force of the solenoid spool rod to generate a pressure difference. Fig. 8 shows the assembly and schematic of the inner configuration of the continuous damping valve.

The main stage determines the valve working range, which is divided into soft, medium, and firm areas, and the soft opening area. The pilot stage influences the maximum pressure quantity and has two functions: bleed control before the transition current and pressure control after the transition current. There is also a method of constructing detailed modeling from the main stage and pilot poppet modeling based on the actual geometry drawing; however, this study adopts an empirical scheme using the pressure vs. flow rate test data from the rig test. The following equation expresses the pressure equation for each of the control current.

$$q_{cdc} = f(\Delta p_{cdc}, i_{cdc}) \tag{4}$$

TABLE 5. Damping force requirements for the active suspension (design case).

Damper Velocity (m/s)	0.05	0.1	0.3
Soft Pressure (Pa)	$\leq 2\times10^6$	$\leq 3\times10^6$	$\leq 7\times10^6$
Firm Pressure (Pa)	$\geq 20\times10^6$	$\geq 45\times10^6$	$\geq 60\times106$

where i_{cdc} is the current for CDC valve. The figure below shows the current versus valve test and the pressure characteristics for each current. The hydraulic valve characteristics should be adjusted to satisfy the requirements of the active and damping modes. First, the pressure characteristics of the solenoid current for damping control must satisfy the basic CDC damping requirement, and the pressure change with respect to the current should be as linear as possible. The required flow rate in each damper speed range based on the outside dimensions of the damper can be arranged as shown in Table 5. The soft mode was selected based on the damping force of the target vehicle to satisfy the external dimensions of the damper and ride comfort. The excitation test conditions of 0.05, 0.1, and 0.3 m/s are defined as the main operating speeds for the damping force evaluation. The criterion for selecting valve characteristics to be in firm mode is that the minimum leakage for the smooth operation of the pump should be at a low speed (0.05 m/s). Also, maximum pressure between $0.05 \sim 0.1$ m/s ranges should be above the pump's mechanical power. The requirement of the valve pressure-flow limit was designed to be more than 45×10^6 Pa at 4.61 lpm at 0.1 m/s. The following table 5 shows the damping force requirements for the active suspension.

The figure below shows the experimental hydraulic power characteristics of the CDC valve in terms of pressure and flow rate. It can be observed that the pressure-to-flow requirements are met, and the hysteresis characteristic is also shown at the 3σ level. The hysteresis characteristic of pressure is an important design criterion because it depends not only on the actual damping force but also on the active force resolution that is to be generated.

B. ACTIVE MOTOR PUMP

For gerotor pumps, dynamic, internal gears, chamber flow rate variations, inlet, and outlet flow modeling are required, and each flow can be calculated using geometric-based modeling. The volume change in each chamber can be modeled as a hydraulic cylinder, and the volume change in the cylinder can be calculated using the volume change curve described above. The pressure difference was set to load by modeling the variable orifices on the inlet and outlet sides. The gerotor leakage phenomenon includes tooth and plate leakage. This parameter can be defined by using a component unit test and correlation. After considering each chamber's initial phase difference characteristics and the total number of chambers, the gerotor dynamic characteristics can be calculated [21].

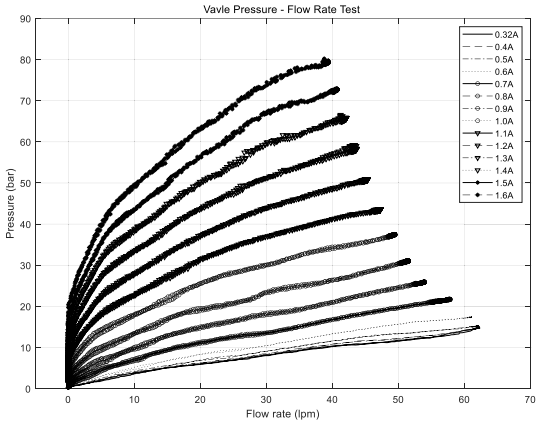

FIGURE 9. Variable valve pressure-flow characteristics (test result).

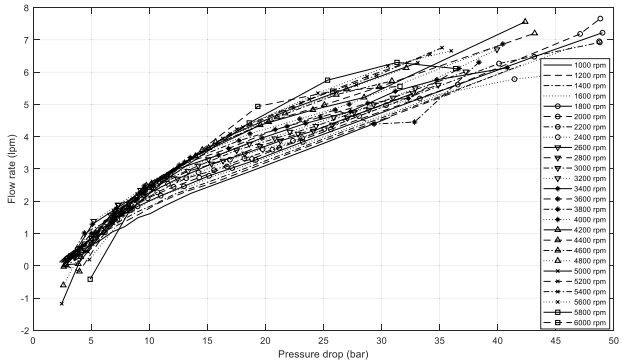

FIGURE 10. Features of the gerotor motor pump leak characteristics.

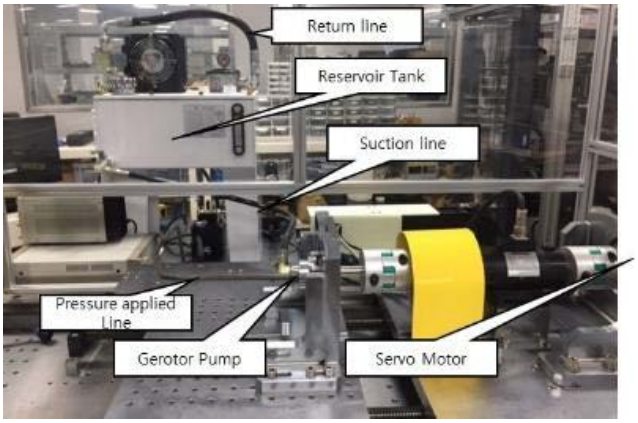

FIGURE 11. Features of the gerotor motor pump leak characteristics and test configuration.

TABLE 6. Gerotor pump main design parameters.

Specification	Unit	parameters
Volumetric displacement	cc/rev	4
No. Outer Lobes	-	7
Shaft Diameter	mm	12
Rotor Tip Clearance	mm	0.07
Outer rotor Diameter	mm	40
Rotor thickness	mm	14.2
Axial thickness	mm	0.05

Modeling has the advantage of considering detailed pump pulsation characteristics, but simplified modeling is applied in this research for the overall control system performance analysis. The pump capacity was used as the design parameter of the model, and the leakage component was modeled using the experimental data. The figure below shows the experimental data of the pump leakage characteristics and simplified modeling by considering the leakage characteristics as an average value. Fig. 10 shows the experimental data of the pump leakage characteristics and simplified modeling by considering the leakage characteristics as an average value. Fig. 10 shows the fluid leakage test results for various pressure load cases.

MOTOR PUMP SYSTEM IDENTIFICATION

The motor pump system dynamics have an important effect on the system performance when assembled with various components, such as the motor, pump, and operation fluid. Because the motor pump operates in the hydraulic circuit during operation, friction and damping occur. Therefore, the system ID was performed based on the nominal region of system operation to estimate the dynamic moment of inertia and damping coefficient of the motor pump assembly. The parameter was estimated via a linear transfer system identification method using the experimental value with sine sweep excitation of up to 10 Hz based on an active force of 1,000 N, which can be seen as the nominal force region. The estimated moment of inertia was 5.87e-05 kgm^2, and the test result was calculated to be 7.56e-05 kgm^2. This influenced the experiment with additional mechanical inertia as compared to the design specifications of the motor pump. The estimated damping value was 0.0025 Nm/(rad/s). Fig 12 shows the pump system nominal operation range, system dynamic input, and output response for the system ID. The main design parameters for the gerotor pump are described in table 6.

An overall active suspension hydraulic model was constructed based on the element modeling described above, as shown in Fig. 13. Fig. 14 shows the detailed actuator model constructed by AMESim and Simulink. A rig test for the model validation was performed by setting the actuator excitation and actuator control conditions, as shown in Table 7. Fig. 15 shows the actuator model validation result of the active suspension. Overall, the damping force characteristics of the first and third quadrants in the damping force mode are similar, as shown by the analytical model. The maximum active force magnitude difference between the simulation and test results is caused by the pressure loss due to flow resistance and leakage, which is difficult to reflect in the modeling. As these characteristics are highly nonlinear, an additional nonlinear model can be added based on the test

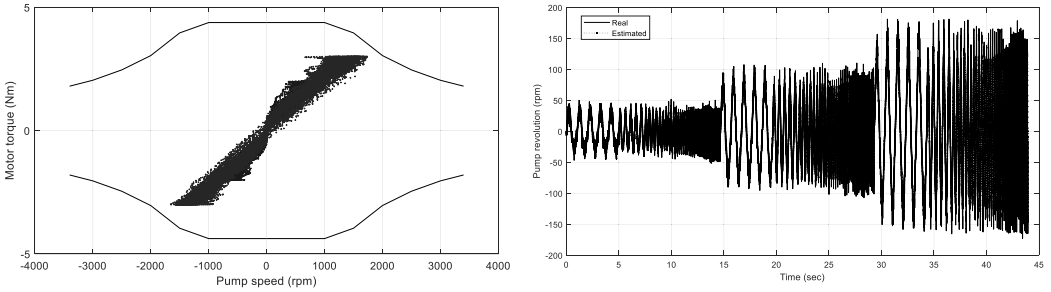

(A) Pump operation region (B) Estimation result (input: torque, output: motor rpm)

FIGURE 12. Features of the gerotor motor pump leak characteristics and test configuration.

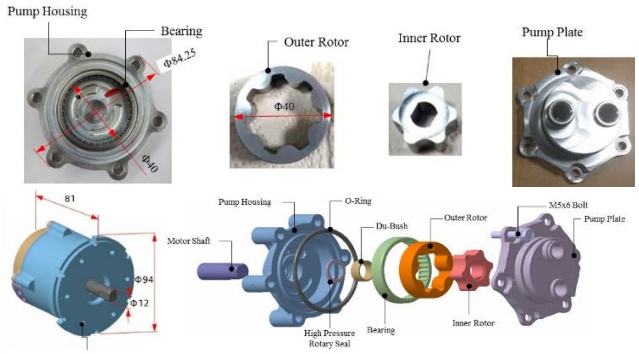

FIGURE 13. Gerotor pump system (components split view).

TABLE 7. Gerotor pump main design parameters.

Damper excitation	(0.05, 0.1, 0.3, 0.6, 1.0, 1.2) m/s
Semi-active Damping Mode	Valve control current apply condition (motor pump is inactive mode) - 0.3, 0.9, 1.6 A
Active Force Control Mode	Valve control is firm mode to create active force - Motor target torque = ± 4 Nm

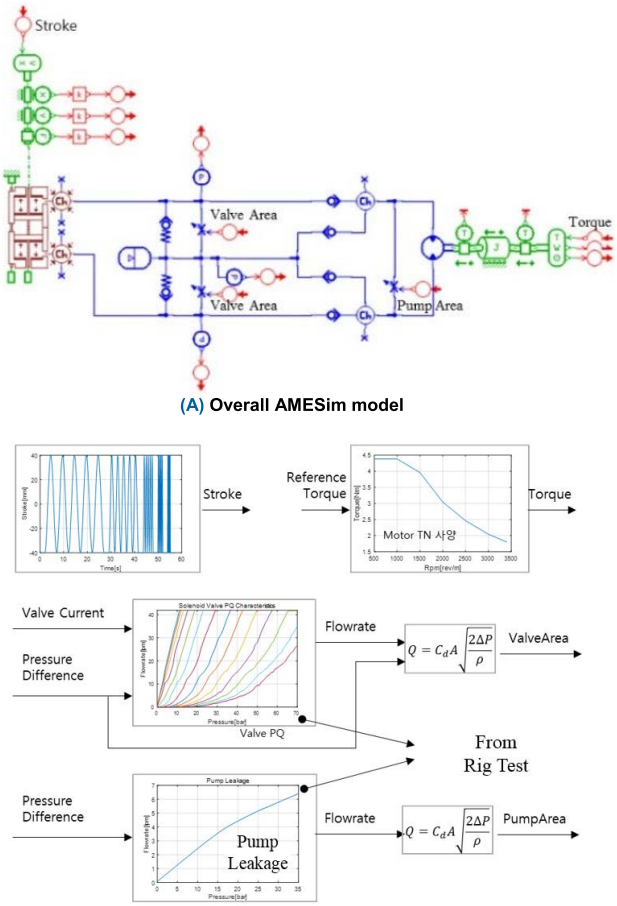

(A) Overall AMESim model (B) Detailed AMESim model explanation

FIGURE 14. Detailed actuator modeling with AMESim and Simulink.

results. However, because this modeling is plant modeling for control system design that considers the actuator's essential nonlinear characteristics, the model's necessary dynamic reliability is considered to have been secured.

V. INTEGRATED CONTROL OF THE ACTIVE SUSPENSION ACTUATOR

Electrohydraulic actuators have a high possibility of performance degradation when tracking the target force by vehicle upper control logic because of nonlinear actuator characteristics and are affected by hardware performance limitations, such as output limitation. In addition, there are many changes in actuator responsiveness and tracking performance owing to realistic power limitations and actuator internal dynamics performance without proper compensation control. Unlike typical hydraulic actuators, vehicle suspension actuators are generally exposed to stochastic road disturbances; therefore, appropriate verification or systematic complementary design is required. When analyzing the actuator operation based on the motion diagram of the system, the main area of interest for damping control from the perspective of tracking control is the performance of the damping (quadrant one and three quadrants) in the force-velocity phase plot. In this study, damping control and piecewise active force control logic through output state feedback were developed for all the operating areas (one, two, three, and four quadrants).

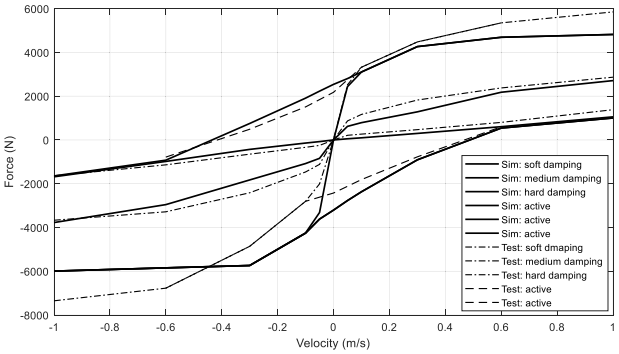

FIGURE 15. Active suspension actuator model validation.

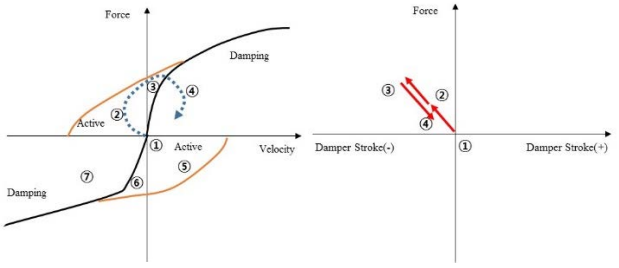

(A) Force versus velocity (B) Force versus displacement

FIGURE 16. Actuator force trajectory during road input.

Vehicle motion can be classified into vertical movement caused by road disturbances and vehicle movement caused by driver input. As shown in Fig. 16, the motion trajectory of the active suspension system was expressed when it passed through the bump. The wheel meets the bumpy road surface, and a compression stroke occurs. Damper motion was controlled to generate more compression strokes for minimizing vehicle body movement. After passing the active area ②, it is switched to the damping area ④ to reduce the rebound motion of the vehicle by damping. The actuator stroke was compressed and then rebounded to return to equilibrium. Therefore, integrated control is important so that there is a seamless force between the active and damping control modes. Regions ⑤ to ⑦ can be thought of as the pothole case, where the same operation pattern is applied. The movement is different from the previous case when vehicle movement occurs owing to the driver's input. Unlike the road input, the driver input is not random. It can generally be regarded as a low-frequency input, as shown in Fig.17. Therefore, the relative speed of the actuator (i.e., damper speed) can be considered as low, and the displacement is relatively large. So the velocity and displacement movement of the damper can be defined as passing from one region ① to the ②. Therefore, in this case, control is applied to actively reduce the magnitude of the vehicle-generated movement through the static active force.

In reviewing the actuator motion plot described above, the actuator functionality should continuously perform variable damping and active force generation. In the damping area (4, 7), the CDC valve is operated to control the damping force, and in the active force generating area (2, 5), active

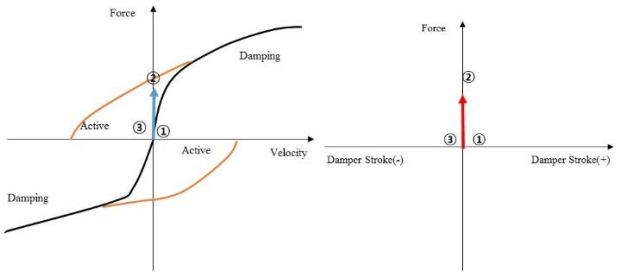

(A) Force versus velocity (B) Force versus displacement

FIGURE 17. Actuator force trajectory during maneuvering.

force control is performed by controlling the pump and valve simultaneously. At this time, CDC valve control should be based on the actuator hydraulic circuit concept so that the pump power can be transmitted to the actuator efficiently. In previous research, the actuator force control was mainly performed only in the damping area control region or the actuator control performance in the area where the active force operation speed is low [8], [24], [25], [26], [27]. In this study, an integrated control of the force control covering the entire operation range was proposed using the CDC valve and motor pump.

The overall actuator control can be expressed as a schematic, as shown in Fig. 18. The total required power of the actuator is determined by the target force, which is calculated using the upper control logic. The logic monitors the operating speed of the motor pump and the flow rate generated by the actuator movement. The current operation point concept calculates the flow rate required to create the required force (pressure). After determining the mode of the vehicle behavior, i.e., passive, semi-active, or active mode, the amount of control required for calculating the required flow rate for the motor and pump actuator is determined.

The next step is to allocate the total power to the pump and semi-active valve. For the pump control side, the motor speed is controlled by considering the pump friction and hydraulic nonlinearity to generate the required pressure. In the CDC valve, solenoid current control performs flow control to generate the required pressure. The pump motor finally performs torque control to control the speed. The entire system architecture was configured as a four-wheel independent motor pump power pack, four-wheel vertical acceleration sensors, and a master ECU structure.

A. INVERSE FORCE MAP BASED CONTROL

If the actuator force characteristic is nonlinear, inverse mapping of the target actuator force using the rig test result is commonly applied in the industry for performance improvement and computation power.

1) SEMI-ACTIVE FORCE CONTROL

The semi-active damping force($F_{semi-active}$) can be calculated as the product of the damper velocity($\dot{x}_s - \dot{x}_{us}$) caused by the

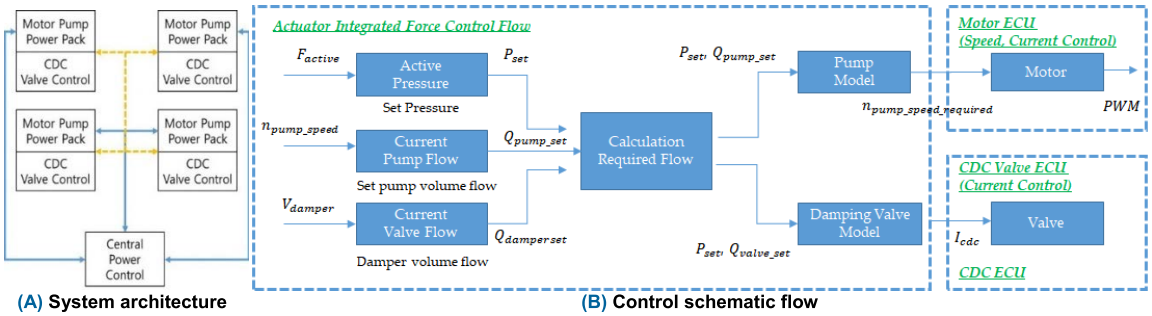

(A) System architecture (B) Control schematic flow

FIGURE 18. Proposed integrated actuator control.

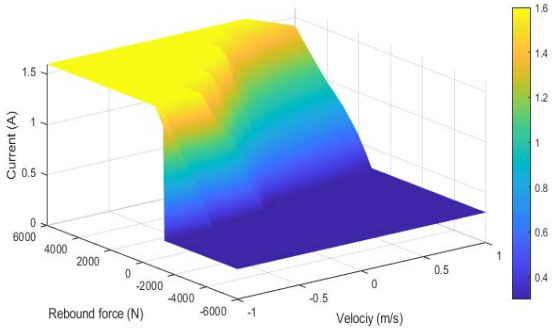

(A) Rebound damping.

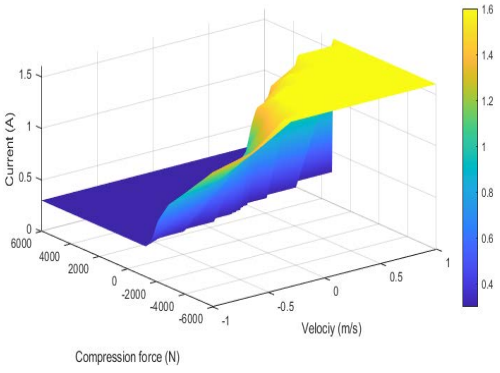

(B) Compression damping.

FIGURE 19. Inverse mapping of damping force characteristics.

disturbance and damping coefficient(c_{cdc}) generated by the control of the solenoid valve. The following Eq. 5 is the equation for calculating of the semi-active damping force. Where $\dot{x}_s$ and $\dot{x}_{us}$ are sprung mass and unsprung mass velocities, respectively.

$$F_{semi-active} = c_{cdc}(\dot{x}_s - \dot{x}_{us}) \tag{5}$$

As shown in Fig. 18, the damping coefficient can be adjusted by controlling the current of the rebound and compression valves. Passive damping characteristics of the actuator can be chosen according to the applied solenoid current $i_{cdc} = [i_{cdc}^{reb} i_{cdc}^{comp}]^T = [0.3A 0.3A]^T$. Although detailed modeling studies on semi-active dampers have been conducted, empirical characteristics for damping control were applied.

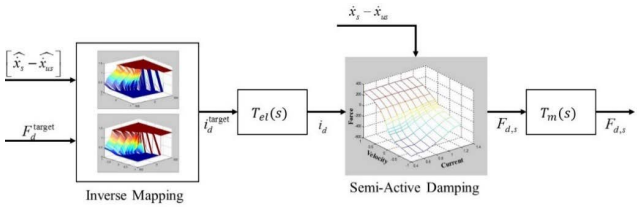

FIGURE 20. Semi-active force control.

The dynamic characteristics are primarily dependent on the hydraulic and solenoid valve characteristics. The influence of the hydraulic dynamics is the time delay related to the oil flow: the bulk modulus and the mechanical inertia term. The experimental results of the hydraulic dynamics varied depending on the damper dimensions and the operating conditions. The electrical characteristics are dependent on the solenoid resistance and inductance characteristics and are set to a 1 ms time response [27], [28]. Fig. 20 shows the block diagram for semi-active force control.

$$T_e(s) = \frac{1}{0.001s + 1}, T_m(s) = \frac{1}{0.02s + 1} \tag{6}$$

2) ACTIVE FORCE CONTROL

Active force is regulated by the motor pump, which generates the flow rate required to build the target pressure inside the actuator. Direct motor torque control is used to generate the required actuator force. Feed-forward-based force control can be conducted using the active force generated by applying the motor torque step-by-step and keeping the velocity constant. The motor dynamics of the electrical and mechanical characteristics are considered by adding a first-order transfer function. Fig. 21 shows the active force characteristics at each motor input torque, and the motor dynamics are described by Eq. 7.

$$T_{motor}(s) = \frac{1}{\tau_{me}s + 1}, \quad \tau_{me} = L/R,$$
$$T_{pump}(s) = \frac{1}{\tau_p s + 1}, \quad \tau_p = J/k_f \tag{7}$$

where L is the inductance and R is the resistance of the motor. J is the total moment of inertia of the motor pump assembly,

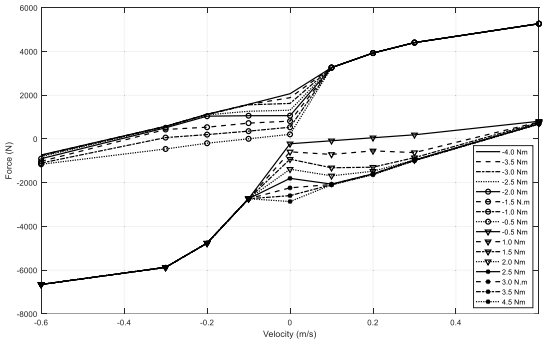

FIGURE 21. Active force characteristics at each motor input torque.

TABLE 8. Active force step response test results.

Velocity (m/s)	Extension Response Time (ms)		Compression Response Time (ms)	
	Soft→Hard	Hard→Soft	Soft→Hard	Hard→Sort
0.1	20	22	27	28
0.2	24	20	32	24
0.3	42	22	41	23

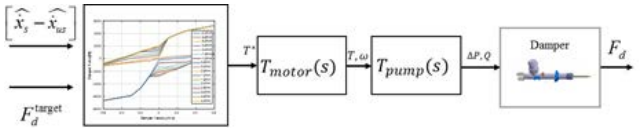

FIGURE 22. Dynamic active feedforward control via motor pump.

and k_f is the friction damping coefficient, which depends on the operating speed and load conditions. The parameters can be estimated using the system ID methodology. Table 8 presents the results of the active-force test on the rig. At low speeds, the response time is up to 20 ms, but as the excitation speed increases, the response becomes slower. As the damper speed is increased, unlike in the damping mode, fast flow compensation using a motor pump is required, but the motor power output is limited with respect to the motor operating speed. Fig. 22 shows the block diagram of dynamic active feedforward control via the motor pump.

B. NONLINEAR MODEL-BASED FORCE

The force control method described in the previous section proposed a method for inverse-map-based feed-forward control using data tested in the nominal operating area of the actuator for target force control. It is advantageous to implement actuator force control logic without additional internal actuator information by performing feed-forward control using the final output characteristics of the actuator. However, because the rig test conditions cannot be representative of all road conditions, there is a limit to satisfying the force tracking performance in real road cases. Therefore, this study applied feedback control based on an actuator-model-based control scheme [20]. The target control input for generating pressure acting on each chamber is calculated based on the actuator system dynamics model, and additional measurement-based feedback control is performed to secure a force tracking performance that is robust against disturbances.

1) ACTIVE FORCE CONTROL

The forces generated by the actuator can be classified into three main categories: forces generated by internal hydraulic pressure($F_{hydraulic}$), forces generated by friction(F_{fric}), and forces generated by inertia(F_{in}).

$$F_a = F_{hyraulic} + F_{fric} + F_{in} \tag{8}$$

Friction is defined as the force generated when an actuator is operated at a slow speed. If the applied force is greater than the friction force, the actuator is set into motion. $F_{dynamic}$ is a frictional force proportional to the excitation velocity and can be applied linearly.

$$\begin{aligned} F_{fric} &= F_{static} + F_{dynamic} \\ F_{dynamic} &= C_{fric}(\dot{x}_s - \dot{x}_{us}) \end{aligned} \tag{9}$$

Inertial forces are generated by the actuator weight and actuator relative acceleration. If the excitation speed is not high, the influence on the overall force of the actuator may be small; however, consideration should be given to the high relative speed, which may affect the force control performance.

$$F_{inertia} = m_{act}(\ddot{x}_s - \ddot{x}_{us}) \tag{10}$$

Hydraulic force can be defined as follows.

$$F_{hyd} = P_{reb}A_{reb} - P_{comp}A_{comp} - F_{offset} \tag{11}$$

F_{offset} is the pre-load applied to the actuator due to the internal pressure.

2) CONTROL STRATEGY OF THE ACTUATOR FORCE

In real operation situations, the actuator dynamics have nonlinear characteristics and limited bandwidth. Therefore, to achieve control of the accurate force in a given stochastic disturbance, it is necessary to derive a nonlinear model-based control and compose a feedback controller to compensate for the model uncertainty and parameter non-linearity. Figure 23 shows the overall nonlinear actuator force control scheme via the force feedback control.

The decision of the operation mode was made based on the target force generated by the upper vehicle controller and the current damper operating speed. A disturbance controller is used using the derivative of the disturbance input x_{damper} and the appropriate low-pass filter transfer function.

$$K_{\text{disturbance}} = sG_d(s)x_{\text{damper}} \tag{12}$$

As shown in Fig. 23, the reference flow rate can be calculated using the nonlinear actuator model and converted into each of the assigned actuator control inputs. The reference motor speed becomes the control target when controlling the motor pump. The speed controller can compensate for uncertainties, such as system inertia and friction, by performing fast control in conjunction with the motor control cycle. Because

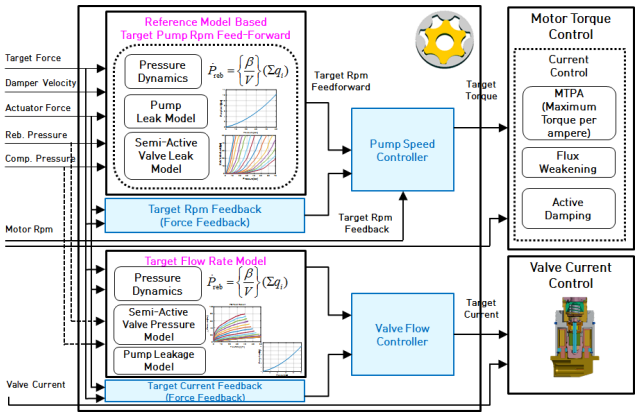

FIGURE 23. Nonlinear actuator pressure dynamics model based force feedback control block diagram.

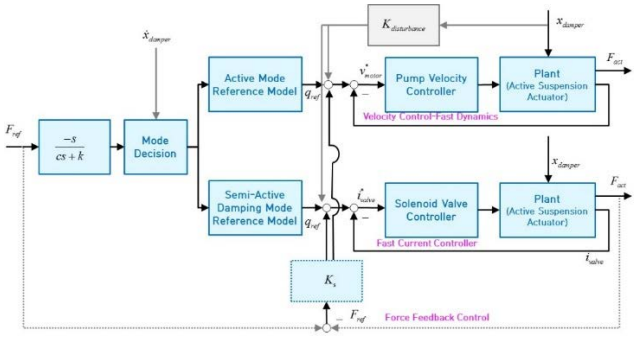

FIGURE 24. Model-based force control flow.

the pressure sensor for each working chamber is installed, the additional uncertainty that is not reflected in the model-based control can be compensated for using a force feedback controller with a low control bandwidth. In addition, to configure the nonlinear controller, a time-varying control design scheme was applied as follows:

$$\dot{\mathbf{x}}_{\text{actuator}} = \mathbf{A}(\boldsymbol{\xi}(t))\mathbf{x} + \mathbf{B}(\boldsymbol{\xi}(t))\mathbf{u}$$
$$\boldsymbol{\xi}(t) = \begin{bmatrix} f_{\text{reb}}(\Delta p, i_{reb}) & f_{\text{comp}}(\Delta p, i_{comp}) & f_{\text{pump}}(\Delta p) \end{bmatrix}^{\mathbf{T}} \tag{13}$$

where A and B in Eq. 13 are the system and input functions, where x and u are state and input vectors, respectively. The pressure dynamics in the actuator internal chamber caused by road disturbances can be summarized as follows:

$$\begin{aligned} \dot{p}_{reb} &= \frac{\beta}{V}(q_{in}^{reb} - q_{out}^{reb}) \\ &= \frac{\beta}{V}(A_{reb}\dot{x}_{damper} - q_{cdc}^{reb} + q_{rpm} - q_{leak}^{reb}) \end{aligned} \tag{14}$$

And compression chamber pressure dynamics of the system can be derived in the same way in (15)–(17), as shown at the bottom of the next page, where β and V are the bulk modulus and volume of the hydraulic system, respectively, and $C_i (i = 1, 2, \ldots, 6)$ is conversion coefficient from pressure to flow rate. The system pressure dynamics can be expressed in terms of flow, and the relative speed of the damper is given by road input. Each component target flows calculation has nonlinear features; therefore, it can be modeled based on the unit semi-empirical experiment. The target flow rate of the motor

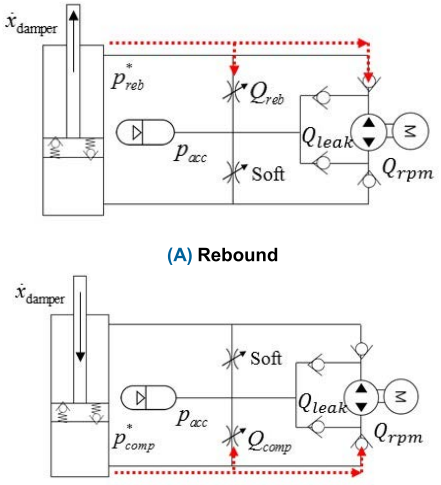

FIGURE 25. Actuator fluid flow (semi-active mode).

and valve, which are the main control inputs, can be obtained from the system state equation, and this can be applied as the feed-forward control terms for the following step control.

The overall control input can be defined as the feed-forward control amount based on the target flow rate derived from the system equation and the PID control based feed-back term calculated based on the actual force error as shown in the equation below. The F_{error} is defined as difference between reference value and measured value.

$$\mathbf{u}(s) = \mathbf{q}_{t\,\text{arg}\,et}^{feed-foward}(s) + (K_p + {}^{K_i}/_{s} + K_d s)F_{error}(s) \tag{18}$$

3) MODEL-BASED SEMI-ACTIVE DAMPING CONTROL

The pressure dynamics in the actuator internal chamber caused by road disturbances can be summarized as follows:

$$\begin{aligned} \mathbf{x}_{\text{actuator}}^{\text{semi-active}} &= \begin{bmatrix} P_{\text{reb}} & P_{\text{comp}} \end{bmatrix}^T \\ \mathbf{u}_{\text{control}}^{\text{semi-active}} &= \begin{bmatrix} I_{\text{valve}} & \dot{x}_{\text{damper}} \end{bmatrix}^T \\ y_{\text{control}}^{\text{semi-active}} &= [F_{\text{active}}]^T \end{aligned} \tag{19}$$

The actuator target force can be expressed using Eq. 20; therefore, the target pressure was calculated based on the target force.

$$\begin{aligned} F^* &= P_{reb}A_{reb} - P_{comp}A_{comp} - F_{offset} \\ P_{reb}^* &= \frac{P_{comp}A_{comp} + F_{offset} + F^*}{A_{reb}} \end{aligned} \tag{20}$$

Based on the target pressure, the internal pressure state equation of the actuator assumes that no pump-side flow occurs in semi-active mode.

$$\begin{aligned} &Q_{rpm}, Q_{leak} = 0 \\ &\dot{P}_{reb} = \frac{\beta}{V_{reb}}(A_{reb}\dot{x}_{damper} + Q_{cdc,reb}) = \frac{P_{reb}^* - P_{reb}}{dt} \end{aligned} \tag{21}$$

The required flow rate at the CDC valve can be derived as follows: If the current pressure and flow rate are known, the required current can be calculated using the pressure-flow rate inverse map acquired using empirical data.

$$\begin{aligned} Q^*_{cdc,reb} &= -A_{reb}\dot{x}_{damper} + \frac{V_{reb}}{\beta}\left\{\frac{P^*_{reb} - P_{reb}}{dt}\right\} \\ Q^*_{cdc,reb} &= f(\Delta P, i_{cdc,reb}) \\ i_{cdc,reb} &= f(\Delta P, Q^*_{cdc,reb}) \end{aligned} \tag{22}$$

The force error between the target and real forces can be calculated by using the pressure sensor measurements at each rebound and compression side. An additional force feedback PI controller was implemented using the force error between the additional actuator force measurement via the pressure sensor and the target force calculated based on the model.

4) MODEL-BASED ACTIVE FORCE CONTROL

In active mode control, pump dynamics are added to the actuator system dynamics. The system state definition is described in Eq. 23.

$$\begin{aligned} \mathbf{x}^{\text{active}}_{\text{actuator}} &= \begin{bmatrix} P_{\text{reb}} & P_{\text{comp}} & \omega_{pump} \end{bmatrix}^T \\ \mathbf{u}^{\text{active}}_{\text{control}} &= \begin{bmatrix} T_{\text{pump}} & \dot{x}_{\text{damper}} \end{bmatrix}^T \\ y^{\text{active}}_{\text{control}} &= [F_{\text{active}}]^T \end{aligned} \tag{23}$$

The actuator chamber pressure dynamics can be described by Eq. 24; assuming that the pressure control cycle is sufficiently fast, the rate of the pressure change can be replaced by the difference between the current pressure and the required pressure divided by the control period. Therefore, the required flow rate of the pump can be calculated in advance using

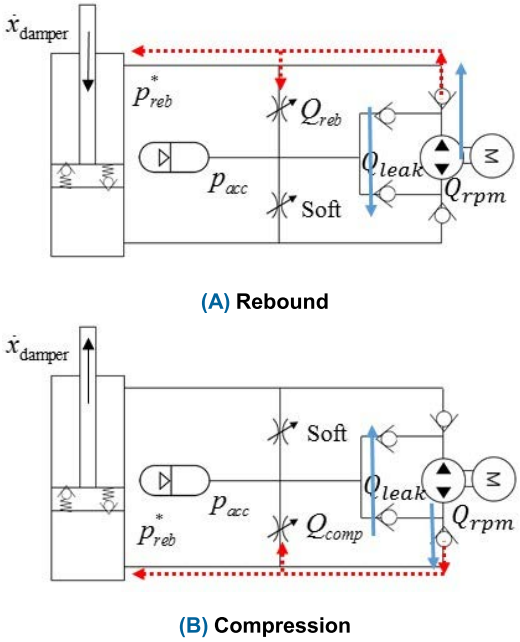

FIGURE 26. Actuator fluid flow (active mode).

the required pressure. The flow rate of the valve and the leakage characteristic of the pump are a result of the pressure difference between the tension chamber and the accumulator, and the pressure drop can be calculated using the non-linear characteristic map. Because the accumulator pressure could not be measured, it was assumed to be the initial neutral pressure. The final target motor speed (rpm) was calculated

$$\begin{aligned} q^{reb}_{cdc} &= f(\Delta p, i_{cdc}) \approx C_1 p_{reb} + C_2 i_{cdc} \\ q^{reb}_{leak} &= f(\Delta p) \approx C_2 p_{reb} \\ q^{reb}_{rpm} &= f(\Delta p) \approx C_{pump} w \\ q^{comp}_{cdc} &= f(\Delta p, i_{cdc}) \approx C_4 p_{comp} + C_5 i_{cdc} \\ q^{comp}_{leak} &= f(\Delta p) = C_6 p_{comp} \\ q^{comp}_{rpm} &= f(\Delta p) = C_{pump} w \end{aligned} \tag{15}$$

$$\begin{aligned} J_{pump}\dot{w} &= T_m - {V_c}/{2\pi}(\Delta p) \\ &= T_m - {V_c}/{2\pi}(p_{reb} - p_{comp}) \end{aligned} \tag{16}$$

$$\begin{aligned} \begin{bmatrix} \dot{p}_{reb} \\ \dot{p}_{comp} \\ \dot{w}_{pump} \end{bmatrix} &= \begin{bmatrix} {\beta_{eff}}/{V_{reb}}(-C_1 - C_2) & 0 & 0 \\ 0 & {\beta_{eff}}/{V_{comp}}(-C_4 - C_6) & 0 \\ -{1}/{2\pi J_m} & {1}/{2\pi J_m} & 0 \end{bmatrix} \begin{bmatrix} p_{reb} \\ p_{comp} \\ w_{pump} \end{bmatrix} \\ &+ \begin{bmatrix} {\beta_{eff}}/{V_{reb}}(A_{reb}) & -{\beta_{eff}}/{V_{reb}}(C_2) & {\beta_{eff}}/{V_{reb}}(C_{pump}) \\ {\beta_{eff}}/{V_{comp}}(A_{comp}) & -{\beta_{eff}}/{V_{comp}}(C_6) & -{\beta_{eff}}/{V_{comp}}(C_{pump}) \\ 0 & 0 & 0 \end{bmatrix} \begin{bmatrix} \dot{x}_{damper} \\ i_{cdc} \\ w_{pump} \end{bmatrix} \\ &+ \begin{bmatrix} 0 \\ 0 \\ {T_m}/{J_{pump}} \end{bmatrix} \end{aligned} \tag{17}$$

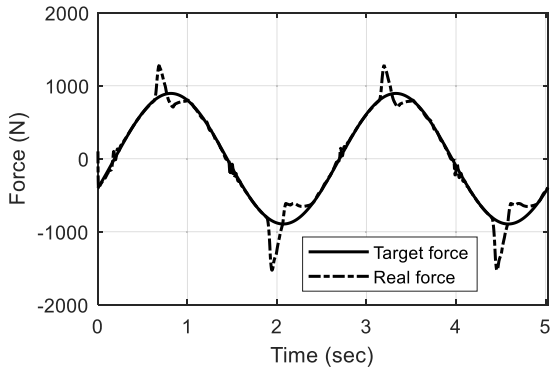

(A) Map based: force tracking performance

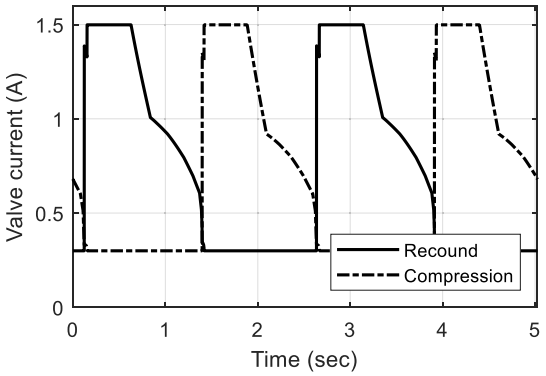

(B) Map-based valve current

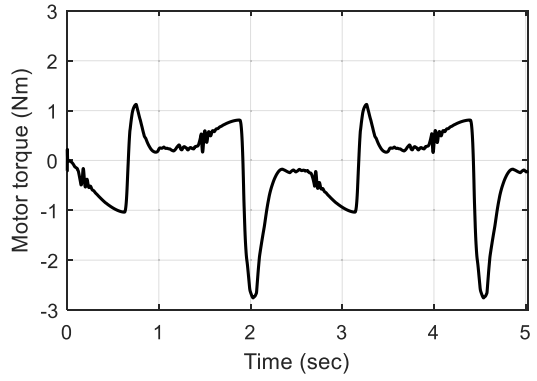

(C) Map based motor torque

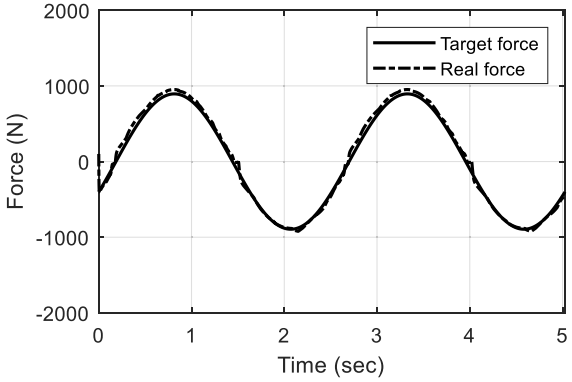

(D) Model-based force tracking performance

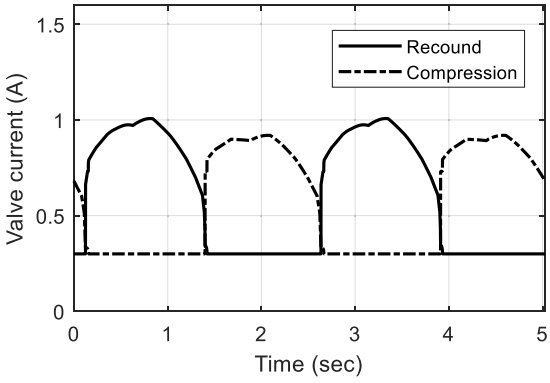

(E) Model-based valve current

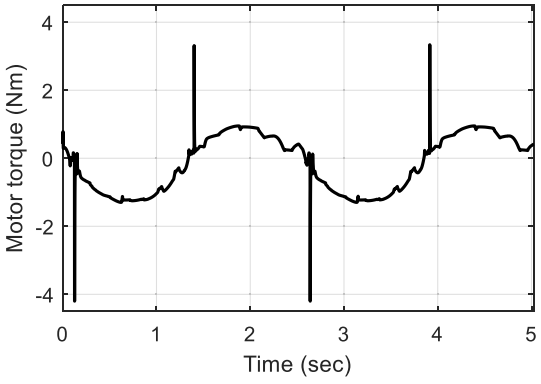

(F) Model-based motor torque.

FIGURE 27. Actuator fluid flow (semi-active mode).

using the volumetric value of the pump.

$$\begin{aligned}\dot{P}_{reb} &= \frac{\beta}{V_{reb}}(A_{reb}\dot{x}_{damper} - Q_{cdc,reb} + Q_{pump} - Q_{leak}) \\ &= \frac{P^*_{reb} - P_{reb}}{dt} \\ Q^*_{pump} &= -A_{reb}\dot{x}_{damper} + Q_{cdc,reb} + Q_{leak} \\ &\quad + \frac{V_{reb}}{\beta}\left\{\frac{P^*_{reb} - P_{reb}}{dt}\right\} \\ &= -A_{reb}\dot{x}_{damper} + f_{cdc,reb}(P^*_{reb}, P_{acc}) \\ &\quad + f_{leak}(P^*_{reb}, P_{acc}) + \frac{V_{reb}}{\beta}\left\{\frac{P^*_{reb} - P_{reb}}{dt}\right\} \end{aligned} \tag{24}$$

Based on the system circuit analysis, maximizing valve control to minimize the pump power loss is possible. However, when switching to semi-active mode, the valve current changes significantly, which may cause a decrease in riding comfort owing to the jerking motion caused by the force mode change. Therefore, the monotonic function is applied to

the force-velocity or pressure-flow rate characteristics of the semi-active force in the active region to improve the jerk such that the force increases with a particular slope in the active mode as the damper speed increases.

VI. SIMULATION AND VALIDATION OF THE ACTUATOR FORCE CONTROL

A. SIMULATION RESULTS

The performances of the proposed model-based force feedback control system and feed-forward map-based semi-active/active integrated control logic were compared. The target force is defined in Eq. 25.

$$F_{t\,\arg\,et} = K_1\dot{x}_{damper} + K_2 x_{damper} \tag{25}$$

As shown in the figure below, the existing inverse map-based control logic shows a force tracking area that does not match the actual situation in the damper speed region. As a result, the tracking deteriorates due to the low-speed region's system dynamics uncertainty. The proposed control concept performs fast control through actuator model-based target rpm control. In addition, the force feedback control based on the pressure sensor measurement signal improves the tracking performance. It can also be observed that the ease of tracking control was improved by reducing instantaneous fluctuations during valve control to reduce the shock generated during valve control.

B. REAL TEST

1) ACTUATOR FORCE CONTROL PERFORMANCE EVALUATION

The experiment was performed in a test rig, as in the simulation input condition. The excitation condition was set at the same damper speed (0.25 m/s 0.8 ∼ 30 Hz) to simulate actuator displacement. The control algorithm was compared with the map-based and model-based force feedback controls proposed in this study.

a: TEST RESULTS OF DAMPING TARGET FORCE TRACKING

The semi-active mode is a case of performing valve control only, and map-based is an inverse map-applied method when in active mode and performing integrated control. The RPM base is the model-based semi-active/active integrated control proposed in this study. In all test regions, it can be observed that the tracking performance is secured up to 12 Hz based on the general phase margin. Therefore, model-based speed control, which is the logic proposed in this study, has better gain and tracking performance.

b: TEST RESULTS OF ACTIVE TARGET-FORCE TRACKING

The effect of the active force on the vehicle decreases as the actuator's operating speed moves toward the high-frequency excitation condition. Therefore, it can be observed that the performance of the proposed control logic is improved up to 5 Hz. This response difference with the semi-active mode can be attributed to the active force module. In addition, the control gain is better, but the phase delay of the tracking performance is similar.

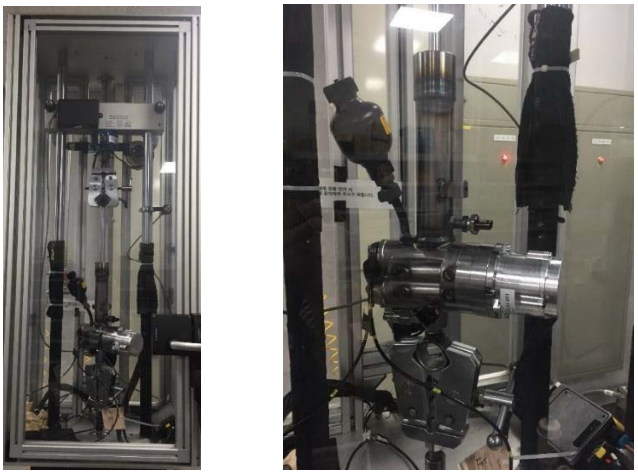

(A) Test rig environment (B) Actuator sample

FIGURE 28. Rig test for the actuator performance evaluation.

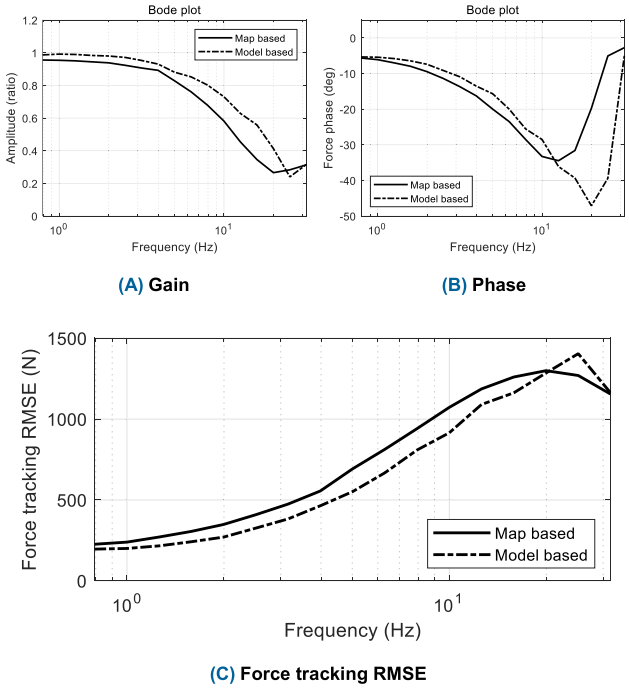

(A) Gain (B) Phase

(C) Force tracking RMSE

FIGURE 29. Actuator performance: damping target force tracking.

2) QUARTER CAR TEST (VEHICLE RIDE CONTROL PERFORMANCE WITH ACTUATOR FORCE CONTROL)

a: TEST RIG SETUP

The test equipment was quarter-car test equipment with a hydraulic excitation actuator. The hydraulic oscillator was manufactured by Schenk and equipped with sprung mass and unsprung mass vertical acceleration sensors to monitor vehicle behavior. In addition, an actuator internal pressure

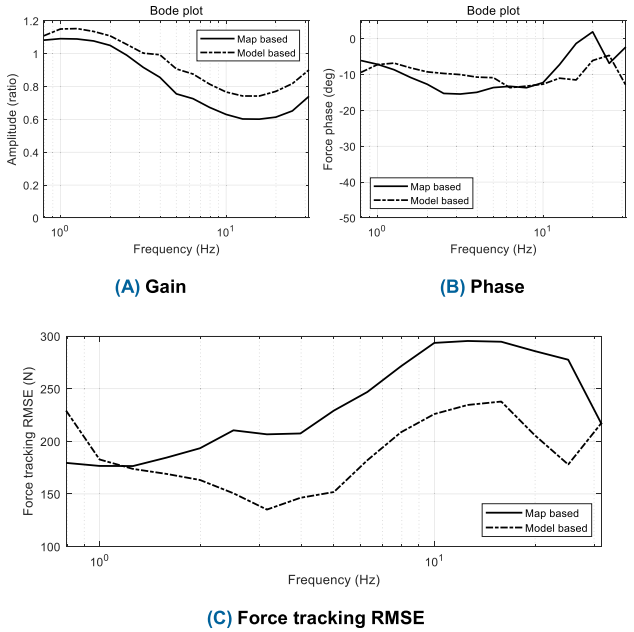

FIGURE 30. Actuator performance: active target force tracking.

FIGURE 31. Quarter-car test rig.

TABLE 9. Vehicle parameters of the quarter car test rig.

Parameters	Value	Unit
Sprung mass	452	Kg
Unsprung mass	68	Kg
Spring stiffness	27,000	N/m
Tire stiffness	200,000	N/m

sensor was mounted in the rebound and compression chamber sections to verify the actuator dynamics.

The actuator control performance evaluation is done by comparing the widely commercialized nonlinear mapping method, which is the concept of applying the actuator force characteristics based on the rig test results, with the performance of the nonlinear model-based force feedback control

TABLE 10. Summary of the performance enhancement index.

Parameters	Performance Index	Map Based (100%)	Proposed (Conventional Control)	Proposed (Skyhook)
Sprung mass	Body G RMS (g)	0.12	0.11 (97%)	0.05 (43%)
	Body G Max (g)	0.39	0.32 (83%)	0.14 (37%)
	Body G Min (g)	-0.35	-0.31 (88%)	-0.16 (45%)
Unsprung mass	Wheel G RMS (g)	0.12	**0.08 (69%)**	**0.11 (91%)**
	Wheel G Max (g)	0.55	**0.42 (76%)**	**0.43 (77%)**
	Wheel G Min (g)	-0.99	**-0.58 (59%)**	**-0.64 (65%)**
Suspension	Stroke RMS (mm)	15.49	12.65 (82%)	8.75 (57%)
	Max Stroke (mm)	43.45	32.31 (74%)	15.55 (36%)
	Min Stroke (mm)	-51.85	-32.69 (63%)	-16.24 (31%)
Actuation Power	Target_Force RMS (N)	197.33	183.25 (93%)	307.99 (249%)
	Power_RMS (Watt)	123.65	25.36 (21%)	85.19 (70%)
	ErrorForce RMS (N)	121.16	54.76 (45%)	89.22 (74%)

proposed in this study. According to the target force tracking performance, it can be seen that in the map-based case, the tracking performance is feasible only in the specific damper speed region and is incorrect in the other actuator operating region. This degraded performance was due to differences in the map test conditions. The actuator control method proposed in this study achieved improved tracking performance through the nonlinear model and then compensated for system uncertainty through feedback control, which significantly improved the target force tracking performance.

$$F_{\text{target}} = -C_1 \dot{x}_{\text{sprung mass}} + B_2(\dot{x}_{\text{sprung mass}} - \dot{x}_{\text{unspurng mass}}) \tag{26}$$

In addition, it can be observed that the current consumption is significantly reduced by not performing unnecessary control generated by the conventional method and by controlling the phase mismatch. In addition, vehicle performance can be affected by the actuator force tracking performance. It can be observed that the change in the unsprung mass dynamics is more significant than that in the sprung mass motion. In the case of the vertical wheel acceleration, the RMS could be reduced by 30% in the test case. The sprung mass motion control with the proposed active damper actuator control scheme was additionally performed and labeled ''Model-Based with Skyhook.'' Therefore, the Applied sprung mass control scheme is the skyhook damping theory defined in Eq. 26.

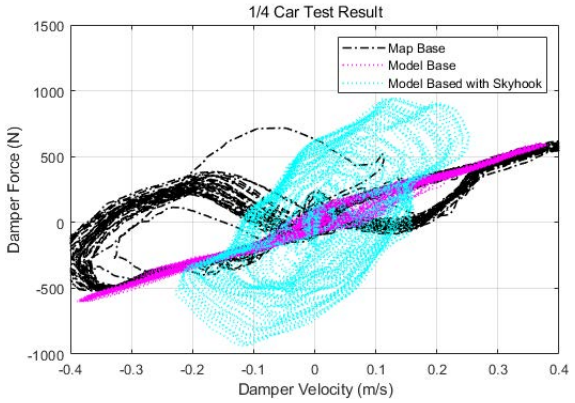

(A) Force tracking

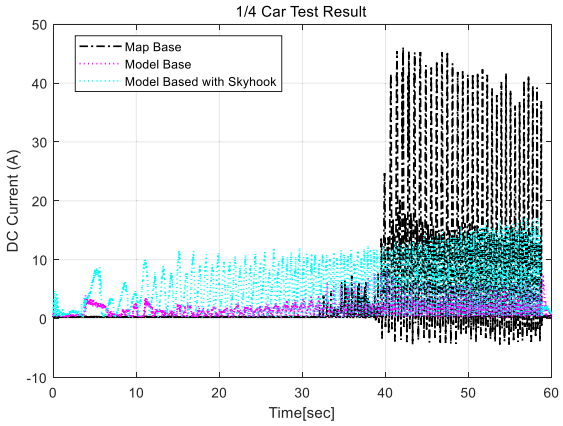

(B) Power consumption

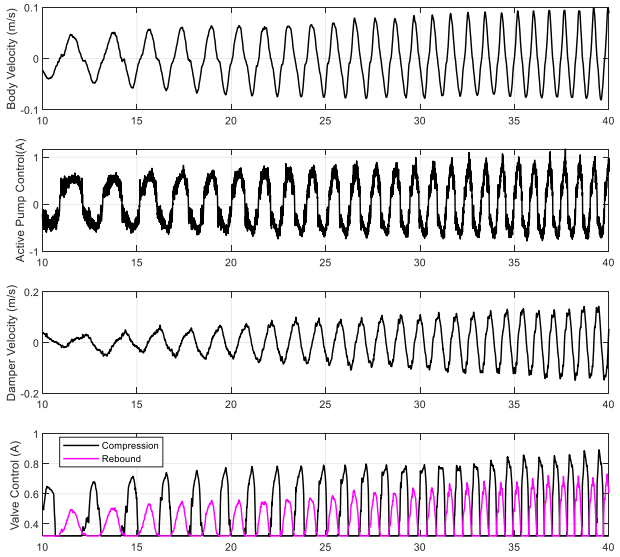

(C) Vehicle Motion with skyhook control inputs

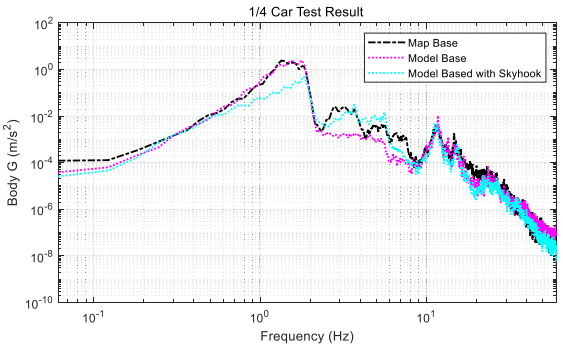

(D) Vertical acceleration of sprung mass

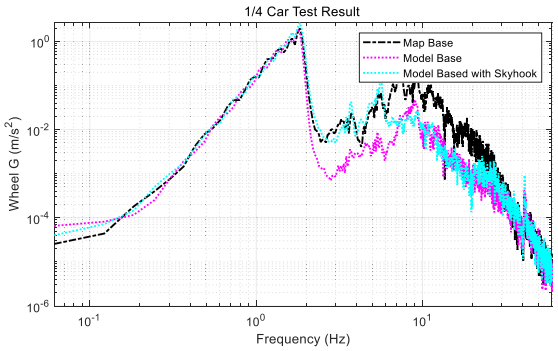

(E) Vertical acceleration unsprung mass

FIGURE 32. Integrated force control performance.

It can be seen that the active force is generated over the entire operating region, as shown in Fig. 32(a). Also, Fig. 32(c) shows that the control input has the same phase with sprung mass vertical velocity. As a result, sprung mass acceleration was reduced around the resonance region, but wheel acceleration performance was similar to the map-base case with a 2∼4Hz region.

Therefore, additional gain scheduling, based on sprung and unsprung mass motion velocity and frequency, can minimize the characteristics of the sprung and unsprung mass

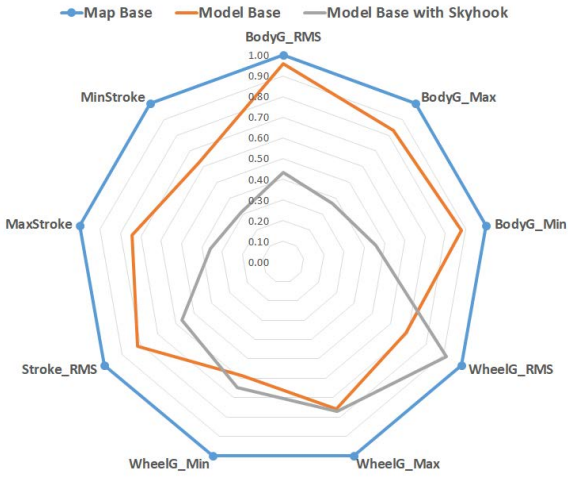

(A) Spider map: vehicle performance indices

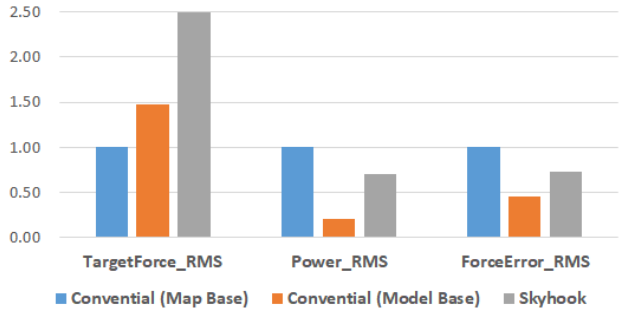

(B) Main benefit of the proposed scheme

FIGURE 33. Performance enhancement index summary.

motion conflict characteristics in terms of ride and handling performance. The actuator tracking force performance with skyhook control seems slightly inferior to the model-based active force control for the target conventional damping force, as shown in Fig.33(b). It can be analyzed that the nonlinear characteristics of the hydraulic system, like the pump and valve operation according to the increase in the target force amplitude and speed, are reflected a little more. Therefore, an adaptive gain scheduling scheme and fine-tuning can improve force tracking performance.

VII. CONCLUSION

This study designed a new decentralized actuator system for cost-effective active suspension actuator control. First, a model-based force control system was proposed and evaluated based on a simulation technique and an actual test platform. Then, to satisfy the existing requirements of traditional automobile damping, it employed an electrohydraulic method and proposed a topology for commercialization. As a result, its structure uses a semi-active damping valve and an active pump module. In addition, a system architecture capable of direct force control using a power source motor pump was selected. Furthermore, we attempted to reduce the system complexity using a gerotor pump, considering the system package and safety as a core part. Finally, verification of the system design for the damping performance and active force generation was performed through system simulation analysis and unit test verification.

An integrated actuator force control algorithm was designed to perform damping and active force functionality in all areas of actuator operation. To perform integrated force control, we developed a model-based actuator-force-control logic that calculates the required flow at the operating point from the total hydraulic power point of view. The control method proposed in this study ensures scalability for various vehicle applications, and reasonable control performance can be sustained using parameter adaptation based on the designed nonlinear characteristics.

In the future, a new upper logic control algorithm for vehicle ride and handling control [28] can be developed by considering the active suspension actuator system performance with data-driven and model-free approaches [29], [30].

REFERENCES

[1] Y. Zhang and A. Alleyne, "A practical and effective approach to active suspension control," *Vehicle Syst. Dyn.*, vol. 43, no. 5, pp. 305–330, May 2005.
[2] M. Satoh, N. Fukushima, Y. Akatsu, I. Fujimura, and K. Fukuyama, "An active suspension employing an electrohydraulic pressure control system," in *Proc. 29th IEEE Conf. Decis. Control*, vol. 4, Dec. 1990, pp. 2226–2231.
[3] T. Merker, G. Girres, and O. Thriemer, "Active body control (ABC) the DaimlerChrysler active suspension and damping system," SAE Tech. Paper 2002-21-0054, 2002.
[4] G. Bismans, "ACOCAR, Fully active wheel and body control," in *Proc. 8th Int. Conf., Adv. Suspension Syst. (IQPC)*, 2016.
[5] *4 pH Technology Development*, Vehicle Dyn. Expo., TNO, The Hague, Netherlands, 2013.
[6] J. Mossberg, Z. Anderson, C. Tucker, and J. Schneider, "Recovering energy from shock absorber motion on heavy duty commercial vehicles," SAE Tech. Paper 2012-01-0814, 2012.
[7] A. Alleyne, "Nonlinear and adaptive control with applications to active suspensions," Doctoral dissertation, Univ. California, Berkeley, Berkeley, CA, USA, 1994.
[8] C. Lauwerys, J. Swevers, and P. Sas, "Robust linear control of an active suspension on a quarter car test-rig," *Control Eng. Pract.*, vol. 13, no. 5, pp. 577–586, 2005.
[9] D. Karnopp, "Active damping in road vehicle suspension systems," *Vehicle Syst. Dyn.*, vol. 12, no. 6, pp. 291–311, Dec. 1983.
[10] E. Katsuyama, "Improvement of ride comfort by triple Skyhook control," in *Proc. 9th Int. Munich Chassis Symp.*, 2018, pp. 215–234.
[11] W. van Casteren Kim, "Robust control of uncertain systems with persistant disturbances," Ph.D. dissertation, Dept. Electron. Elect. Eng., Pohang Univ. Sci. Technol., 2000.
[12] G. Koch, E. Pellegrini, S. Spirk, N. Pletschen, and B. Lohmann, "Actuator control for a hybrid suspension system," Tech. Rep. Autom. Control, Technische Universitat Munchen, Munich, Germany, Tech. Rep. TRAC-6, Dec. 2011.
[13] Y. Zhang and A. Alleyne, "A practical and effective approach to active suspension control," *Vehicle Syst. Dyn.*, vol. 43, no. 5, pp. 305–330, 2005.
[14] K. Reybrouck, B. Vandersmissen, and K. Six, "ACOCAR: Ultimate comfort and safety through the energy-efficient active damping system of Tenneco," in *Proc. 21st Aachen Colloq. Automobile Engine Technol.*, 2012, pp. 1–15.
[15] B. L. J. Gysen, J. J. H. Paulides, J. L. G. Janssen, and E. A. Lomonova, "Active electromagnetic suspension system for improved vehicle dynamics," *IEEE Trans. Veh. Technol.*, vol. 59, no. 3, pp. 1156–1163, Mar. 2010.
[16] C. Braunholz, J. Wiedemann, J. Neubeck, I. Scharfenbaum, U. Schaaf, and A. Wagner, "Active roll stabilization design considering battery-electric vehicle requirements," in *Proc. 26th Aachen Colloquium Automobile Engine Technol.* 2017, p. 2017.

[17] C. Jablonowski, C. Schimmel, and V. Underberg, "The chassis of the all-new AUDI A8," in *Proc. 8th Int. Munich Chassis Symp.* Wiesbaden, Germany: Springer-Vieweg, 2009, pp. 7–26.
[18] B. L. J. Gysen, T. P. J. van der Sande, J. J. H. Paulides, and E. A. Lomonova, "Efficiency of a regenerative direct-drive electromagnetic active suspension," *IEEE Trans. Veh. Technol.*, vol. 60, no. 4, pp. 1384–1393, May 2011.
[19] *Efficient Active Suspension for Mass Production*, Vehicle Dyn. Expo., Clearmotion, Billerica, MA, USA, 2013.
[20] O. Ajala, D. Bestle, and J. Rauh, "Modelling and control of an electro-hydraulic active suspension system," *Arch. Mech. Eng.*, vol. 60, no. 1, pp. 37–54, Mar. 2013.
[21] S. André, "Optimization of valve damping," M.S. thesis, Dept. Manag. Eng. Division Fluid Mechatronic Syst., Linköping Univ., Linköping, Sweden, 2013.
[22] M. Fabiani, S. Manco, N. Nervegna, and M. Rundo, "Modeling and simulation of gerotor gearing in lubricating oil pumps," *SAE Trans.*, vol. 108, no. 3, pp. 989–1003, 1999.
[23] R. Goodall, G. Freudenthaler, and R. Dixon, "Hydraulic actuation technology for full- and semi-active railway suspensions," *Vehicle Syst. Dyn.*, vol. 52, no. 12, pp. 1642–1657, Dec. 2014.
[24] E. Pellegrini, "Model-based damper control for semi-active suspension systems," Doctoral dissertation, Technische Universitat Munchen, Munich, Germany, 2012.
[25] M. Fleps-Dezasse, J. Tobolar, and J. Pitzer, "Modelling and parameter identification of a semi-active vehicle damper," in *Proc. Linköping Electron. Conf.*, Lund, Sweden, Mar. 2014, pp. 283–292.
[26] H. E. Tseng and D. Hrovat, "State of the art survey: Active and semi-active suspension control," *Vehicle Syst. Dyn.*, vol. 53, no. 7, pp. 1034–1062, 2015.
[27] S. Savaresi, C. Vassal, C. Spelta, and O. Sename, *Semi-Active Suspension Control Design for Vehicles*. Amsterdam, The Netherlands: Elsevier, 2010.
[28] H. Basargan, A. Mihály, P. Gáspár, and O. Sename, "Cloud-based adaptive semi-active suspension control for improving driving comfort and road holding," *IFAC-PapersOnLine*, vol. 55, no. 14, pp. 89–94, 2022.
[29] I. Ahmad, X. Ge, and Q.-L. Han, "Decentralized dynamic event-triggered communication and active suspension control of in-wheel motor driven electric vehicles with dynamic damping," *IEEE/CAA J. Automat. Sinica*, vol. 8, no. 5, pp. 971–986, May 2021.
[30] C. Chen, J. Xu, G. Lin, Y. Sun, and F. Ni, "Model identification and nonlinear adaptive control of suspension system of high-speed maglev train," *Vehicle Syst. Dyn.*, vol. 60, no. 3, pp. 884–905, Mar. 2022.

JEONG-WOO LEE received the B.S. and M.S. degrees in mechanical engineering from Pusan National University, South Korea, in 1997 and 1999, respectively, and the Ph.D. degree in mechanical and aerospace engineering from Seoul National University, Seoul, in 2020. His research interests include integrated chassis control systems, electrified active safety systems, and motion control systems for automated driving of ground vehicles.

KWANGSEOK OH (Member, IEEE) received the B.S. degree in mechanical engineering from Hanyang University, Seoul, in 2009, and the M.S. and Ph.D. degrees in mechanical and aerospace engineering from Seoul National University, Seoul, in 2013 and 2016, respectively. From 2016 to 2017, he was an Assistant Professor with the Automotive Engineering Department, Honam University. Since 2017, he has been an Associate Professor with the School of ICT, Robotics and Mechanical Engineering, Hankyong National University, Anseong-si, South Korea. His research interests include fail-safe systems for autonomous driving, adaptive and predictive control, and intelligent control.